Control of grid-connected inverter output current: a practical review

Victor Habermann Avila
Academic Department of Electrotechnics
Federal University of Technology
Curitiba, Brazil
avilahvictor@gmail.com

Vicente Leite
Research Centre in Digitalization and Intelligent Robotics (CeDRI)
Polytechnic Institute of Bragança
Bragança, Portugal
avtl@ipb.pt

***Abstract*— The number of grid-connected inverters is growing due to the expansion of the use of renewable energies (RE) systems and this may affect grid power quality and stability. Some control algorithms reduce injected current harmonics and add new possibilities to the converter. This paper implements and analyses the proportional integral (PI) controller in the synchronous frame and the proportional resonant (PR) controller with and without the harmonics compensators (HC). All these control strategies have proven to be effective and robust. However, the PR+HC controller presents better output current quality. The PI and PR controllers have similar performances. This work also compares the harmonic content of the current with the IEEE 1547 reference and with three commercial inverters from different manufacturers.**

Keywords*— *grid-connected inverter, proportional resonant, synchronous frame, current control

I. INTRODUCTION

The participation of the distributed generation power systems (DGPSs) on the electrical matrix is expanding, especially the ones with RE sources [1, 2]. In the context of DGPSs, electrical vehicles can provide power when connected to the grid if a bidirectional charger topology is adopted [3, 4].

Several alternative controllers have been studied and proposed in the past years due to the drawback of the PI controller to follow *ac* references [5]. One alternative is transforming the *ac* variables of the inverter into *dc* values using *dq* transformation and PI controller, as presented in [4, 5, 6]. The proportional resonant (PR) controller is another solution, where the controller has an infinite gain at a selected resonant frequency and can achieve zero steady state error for *ac* references [9, 10, 11]

The inverter is an essential component of a DGPSs. It is the link between the energy source and the grid. If the inverter is not operating properly, the injected power can cause voltage and frequency oscillations and poor grid power quality. The control algorithms of the inverters are a critical factor to assure that the injected power has low harmonic content and complies with international standards [5, 12]. Some of these, such as the IEEE 1547-2003, determine harmonics limits for the current injected into the grid. The total rated distortion (TRD) is limited to 5% and the *dc* injection limit is 0.5% [13].

This paper analyses the performance, focusing in the harmonics, of the output current controllers applied in a grid connected single-phase inverter. The *dq* frame transformation with PI controller and the PR controller were tested. The output current of some commercial inverters was also analysed and compared with the results obtained with the controllers implemented in the experimental platform.

II. OUTPUT CURRENT CONTROL

Several controllers can be applied to control the output current of inverters. Furthermore, the same controller can be used with variables in different frames to improve its performance. For instance, a simple proportional integral controller can work either in the natural *αβ* frame or in the *dq* frame. To avoid frame transformations, a PR controller is an alternative to the PI controller.

A. PI in the synchronous frame

The use of the *dq* synchronous frame applied to single-phase systems was first introduced in [8]. It proposes the use of an imaginary circuit to have a pair of orthogonal sinusoidal values (e.g. i_α and i_β). With this pair of values, a frame transformation matrix is applied to represent i_α and i_β as *dc* values in a frame that rotates at a synchronous speed. This rotating frame, composed by the direct and quadrature axis, has the same angular speed (ω) of the grid voltage. By this way, a simple PI controller can be used to achieve zero steady state error [5]. Furthermore, if the phase angle for the transformation (θ) is equal to the phase angle of the grid voltage, the direct axis is aligned with the grid voltage vector. This allows independent control of active and reactive powers, as presented in [14]. Fig. 1 presents the block diagram of the control structure chosen for this paper. The reference currents in the *dq* frame are generated by the power references. To obtain the equivalent in the *dq* frame for the output current, it is delayed by 90 degrees and goes through a frame transformation. Then, the *dq* equivalent of the output current is compared with the references and the error goes through a PI controller that will generate the control signal for the inverter PWM.

B. Proportional resonant controller

The PR controller has a similar operation as the PI controller. However, instead of an integrator, the PR has a resonant portion. This results in a frequency shift of the infinite gain from *dc* values, with PI controller, to a given resonance frequency (ω), with PR controller [10]. With that, no frame transformation is required to achieve zero steady-state error for sinusoidal references. Nevertheless, infinite gain may lead to stability problems. Then, a cut-off frequency

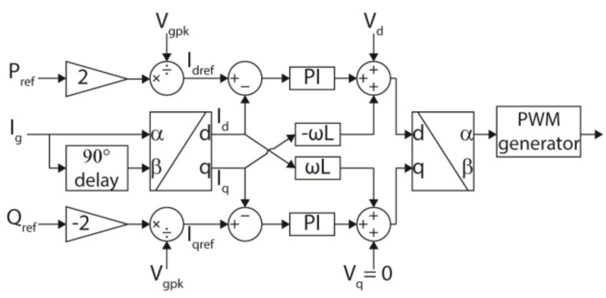

Fig. 1. PI controller in the synchronous frame block diagram.

978-1-7281-7369-6/20/$31.00 ©2020 IEEE

(ω_c) is introduced to limit the gain at the resonant frequency. This results in a more stable system and a widened bandwidth gain. This improves results in applications where the frequency can oscillate around a value, i.e. grid-connected inverters [10]. Equation (1) presents the controller transfer function with a cut-off frequency ω_c . K_P and K_I are the proportional and resonant gain, respectively.

$$G_{PR}(s) = K_{P\_PR} + (2.K_{I\_PR}.\omega_c.s)/(s^2 + 2.\omega_c.s + \omega^2) \quad (1)$$

It is possible to use multiple resonant controllers in parallel, each one tuned at a selected resonant frequency. This allows the harmonic compensation (HC) of the harmonics that can occur in the controlled variable. Fig. 2 presents the control algorithm used to test the PR controller for this paper. The reference current is generated in the *dq* frame, based on the power references. After that, the currents are transformed to the natural frame and the reference is compared to the actual output current of the inverter, the error goes through the PR controller that generates the duty cycle for the inverter PWM. Several improvements of the control structure have been proposed, such as frequency adaptive methods to enhance system stability during frequency oscillations [15] [16] or optimal tuning of controller gains [17].

III. Experimental implementation

The experimental results presented in this work were achieved with the same set-up of [18] [19]. It is a bidirectional *dc-ac* power topology with a bidirectional *dc-dc* converter and a full bridge inverter, presented in Fig. 3. It can be used for several applications, such as vehicle-to-grid (V2G) or grid-to-vehicle (G2V). This work used the V2G operation mode, where the first stage operates as a boost converter with a battery bank (8x12 V) as input, a *dc*-link capacitor (1 mF) and a voltage source inverter connected to the grid through an LC filter (5.6 mH, 1 μF). The whole topology is based on the Powerex PM75RLA120 intelligent power module. The dSPACE DS1103 real-time controller board was used along with a Simulink® and ControlDesk® application to evaluate the control algorithms. The experimental setup used for the tests is depicted in Fig. 4.

Table I presents the selected gains for the PI controller in the *dq* frame and for the PR controller, the HC gain is equal to K_{I_PR}, the resonant frequency (ω) is 340 rad/s and the cut-off frequency (ω_c) is 1 rad/s.

TABLE I CONTROLLERS GAINS FOR THE TESTS.

K_{P_PI}	K_{I_PI}	K_{P_PR}	K_{I_PR}
20	1000	25	750

IV. Results and discussion

Extensive testing was made to evaluate controller performance at different injected power levels. It was tested the PR controller (Fig. 5), PR controller with compensation of the 3rd, 5th and 7th harmonics (Fig. 6) and the PI controller in

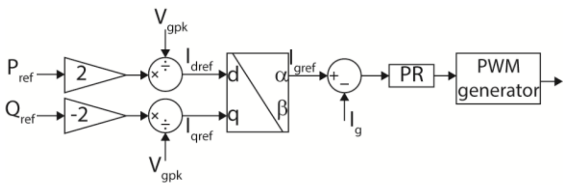

Fig. 2. PR controller block diagram

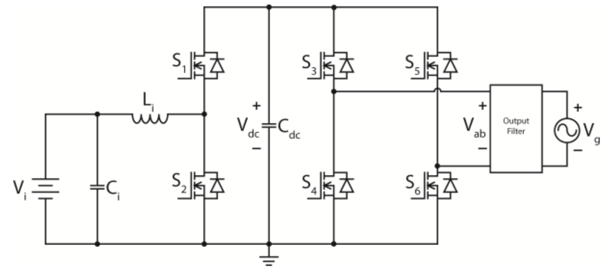

Fig. 3. Bidirectional topology used

the *dq* frame (Fig. 7). All three controllers had a current in phase with the grid voltage and with some distortion in some frequencies. Both PR and *dq* frame controllers had a significant distortion caused by the third harmonic, effect that is mitigated with the HC.

The effects of the controllers in the harmonics can be visualized better in the harmonic spectrum of the output current, presented in Fig. 8. It presents the harmonics for the three tested controllers and the individual limits specified by IEEE 1547. Now it is easier to see that the PR and *dq* controllers have high harmonic content in the 3rd, 5th and 7th harmonics, where the limits are violated. The HC effectively reduced these values to satisfy the limits of the standard. However, all three controllers did not satisfy the limits of 11th and 13th harmonics.

To analyse the behaviour of the controllers with the variation of the injected power it was also acquired the output current for the controllers when injecting half of the rated power (500 W), presented in Fig. 9 to Fig. 11

Table II presents the inverter output current *rms* value, (I_{g_rms}), output power (P_o) and total harmonic distortion (THD) for the three tested controllers.

Along with that, the output current of three commercial inverters, from distinct companies, was measured for comparison purposes. It was tested the Kostal PIKO MP Plus 1.5-1 (Rated power: 1500 W), the SMA Sunny Boy 1.5-1VL-40 (Rated power: 1500 W) and the Ginlong Solis mini 700 (Rated power: 700 W). The harmonic spectrum of these inverters is presented in Fig. 12 According to the tests performed, the Kostal PIKO and Ginlong Solis respected all individual harmonics limits and SMA Sunny Boy surpassed the 5th and 7th limits Table III presents the inverter output current *rms* value (I_{g_rms}), output power (P_o) and total harmonic distortion (THD) for the three tested commercial inverters.

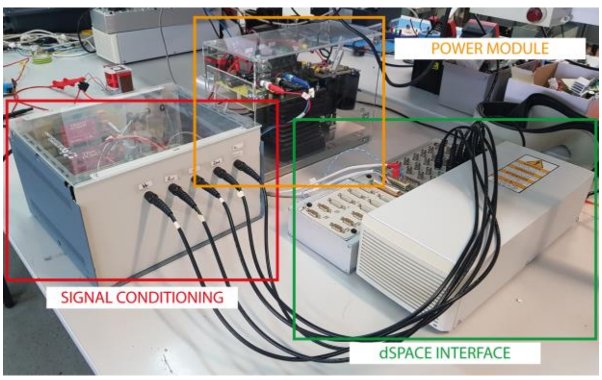

Fig. 4 - Experimental platform used for the tests

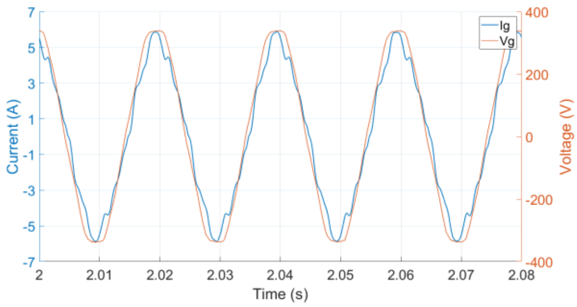

Fig. 5. Output for PR controller - P_{ref} = 1000 W

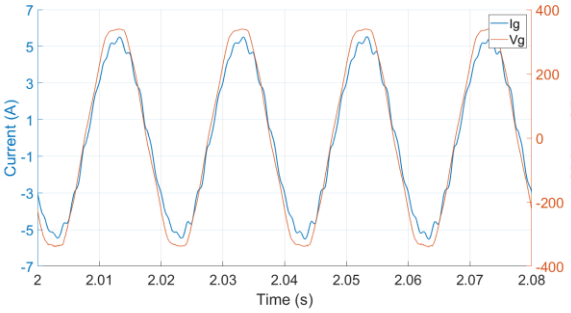

Fig. 6. Output for PR+HC controller - P_{ref} = 1000 W

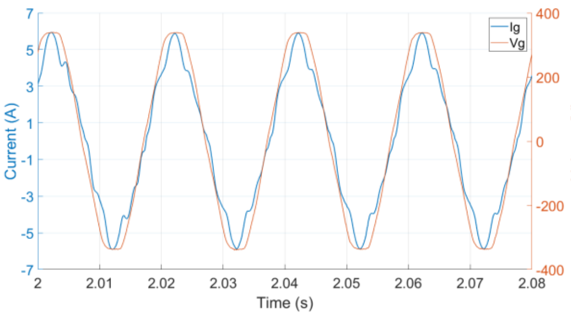

Fig. 7. Output for *dq* controller - P_{ref} = 1000 W

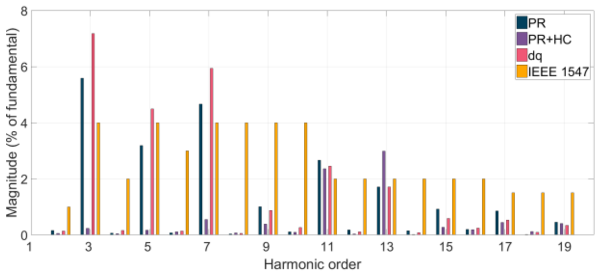

Fig. 8. Harmonics for different controllers

TABLE II OUTPUT VALUES FOR DIFFERENT CONTROLLERS

Controller	I_{g_rms} (A)	P_o (W)	THD (%)
PR	3.72	918.30	9.02
	1.71	417.54	16.92
PR+HC$_I$	3.70	912.49	4.34
	1.68	409.35	8.04
PI	3.66	903.32	11.26
	2.04	499.01	18.10

Regarding the results from the tested controllers, the PR with HC had the best results. However, each harmonic compensator added may increase the computational cost of the controller, which may not be viable in some situations. The PI in *dq* frame and PR controllers did not satisfy all IEEE 1547 limits. Thus, it can also be used in simpler applications and with improved output filters to reduce some harmonics.

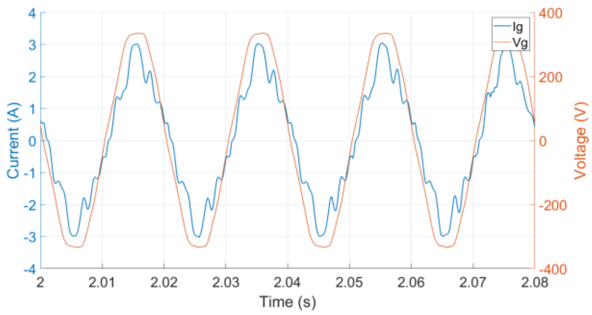

Fig. 9. Output for PR+HC controller - P_{ref} = 500 W

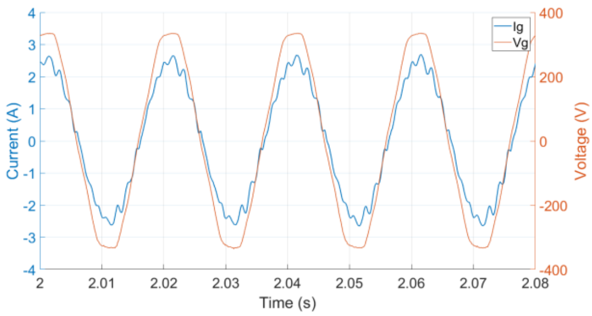

Fig. 10. Output for PR+HC controller - P_{ref} = 500 W

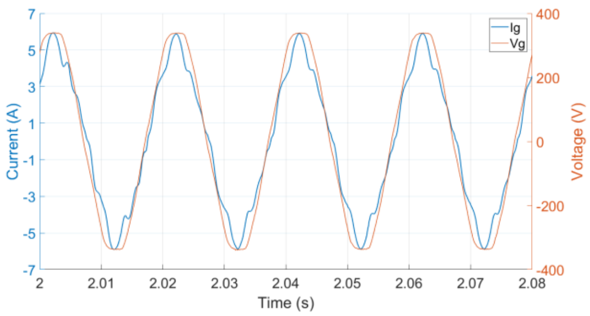

Fig. 11. Output for dq controller - P_{ref} = 500 W

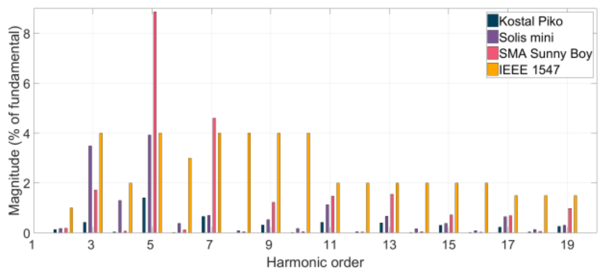

Fig. 12. Harmonics for commercial inverters

TABLE III OUTPUT VALUES FOR COMMERCIAL INVERTERS

Controller	I_{g_rms} (A)	P_o (W)	THD (%)
Kostal PIKO	4.32	1041.50	3.81
Ginlong Solis$_I$	3.13	751.45	5.88
SMA Sunny Boy	3.84	928.54	10.69

Analyzing the output values of the commercial inverters, both crossed the THD limits (Ginlong Solis and SMA Sunny Boy). However, the Sunny Boy was not tested in the rated power. It is important to mention that all tested inverters are certified and are available in the market. The Kostal PIKO, even it was not tested in rated power respected all IEEE 1547 limits.

V. CONCLUSION

The number of inverters injecting power to the grid is increasing and is important to assure good quality to the generated power. Then, output current control algorithms have an important role in this scenario. The PI controller in the *dq* reference frame and PR controller are two of the most common control algorithms used to control the output current of grid connected inverters. In this work, both controllers were implemented, and the results compared with the output current of commercial inverters.

The PR controller with harmonic compensation presented the best results with low THD and limiting the individual harmonics that were compensated. However, this type of controller takes computational cost and this factor may be analyzed before application. The PR controller and *dq* frame controller presented results over the limits of the standards, but with auxiliary controllers or other types of output filter these results can be improved.

With the reduction of the injected power, the THD increased due to the gains of the controller. To the inverter operate in the best condition the gains must be adjusted to each power value. However, this is not simple to apply.

REFERENCES

[1] A. Timbus, M. Liserre, R. Teodorescu, P. Rodriguez and F. Blaabjerg, “Evaluation of current controllers for distributed power generation systems,” *IEEE Transactions on power electronics,* vol. 24, no. 3, pp. 654--664, 2009.

[2] M. Zainuddin, F. E. P. Surusa, S. Syafaruddin and S. Manjang, “Constant Power Factor Mode of Grid-Connected Photovoltaic Inverter for Harmonics Distortion Assessment,” *International Journal of Renewable Energy Research,* vol. 10, no. 3, pp. 1525-1535, 2020.

[3] A. Sharma and S. Sharma, “Review of power electronics in vehicle-to-grid systems,” *Journal of Energy Storage,* vol. 21, pp. 337--361, 2019.

[4] N. Sujitha and S. Krithiga, “Grid tied PV-Electric Vehicle Battery Charger using Bidirectional Converter,” *International Journal of Renewable Energy Research,* vol. 9, no. 4, pp. 1873-1881, 2019.

[5] F. Blaabjerg, R. Teodorescu, M. Liserre and A. V. Timbus, "Overview of control and grid synchronization for distributed power generation systems," *IEEE Transactions on industrial electronics,* vol. 53, no. 5, pp. 1398--1409, 2006.

[6] M. Ebrahimi, S. A. Khajehoddin and M. Karimi-Ghartemani, “Fast and robust single-phase DQ current controller for smart inverter applications,” *IEEE transactions on power electronics,* vol. 31, no. 5, pp. 3968--3976, 2015.

[7] B. Crowhurst, E. El-Saadany, L. El Chaar and L. Lamont, "Single-phase grid-tie inverter control using DQ transform for active and reactive load power compensation," in *2010 IEEE International Conference on Power and Energy*, 2010.

[8] R. Zhang, M. Cardinal, P. Szczesny and M. Dame, “A grid simulator with control of single-phase power converters in DQ rotating frame,” in *2002 IEEE 33rd Annual IEEE Power Electronics Specialists Conference*, 2002.

[9] N. Zhang, H. Tang and C. Yao, “A systematic method for designing a PR controller and active damping of the LCL filter for single-phase grid-connected PV inverters,” *Energies,* vol. 7, no. 6, pp. 3934--3954, 2014.

[10] R. Teodorescu, F. Blaabjerg, M. Liserre and P. C. Loh, "Proportional-resonant controllers and filters for grid-connected voltage-source converters," *IEE Proceedings-Electric Power Applications,* vol. 153, no. 5, pp. 750--762, 2006.

[11] A. G. Yepes, F. D. Freijedo, J. Doval-Gandoy, O. Lopez, J. Malvar and P. Fernandez-Comesana, “On the discrete-time implementation of resonant controllers for active power filters,” in *2009 35th Annual Conference of IEEE Industrial Electronics*, 2009.

[12] M. a. M. M. Najeeb, R. Razali, H. Daniyal and J. A. Yahaya, “Experimental implementation controlled SPWM inverter based harmony search algorithm,” *International Journal of Renewable Energy Research,* vol. 7, no. 3, pp. 1041-1052, 2017.

[13] R. C. Dugan, T. S. Key and G. J. Ball, "Distributed resources standards," *IEEE Industry Applications Magazine,* vol. 12, no. 1, pp. 27--34, 2006.

[14] S. Samerchur, S. Premrudeepreechacharn, Y. Kumsuwun and K. Higuchi, “Power control of single-phase voltage source inverter for grid-connected photovoltaic systems,” in *2011 IEEE/PES Power Systems Conference and Exposition*, 2011.

[15] K. Seifi and M. Moallem, "An adaptive PR controller for synchronizing grid-connected inverters," *IEEE Transactions on Industrial Electronic,* vol. 66, no. 3, pp. 2034--2043, 2018.

[16] Y. a. Z. K. Yang, H. Wang, F. Blaabjerg, D. Wang and B. Zhang, "Frequency Adaptive Selective Harmonic Control for Grid-Connected Inverters," *IEEE Transactions on Power Electronics,* vol. 30, no. 7, pp. 3912--3924, 2014.

[17] O. Husev, C. Roncero-Clemente, E. Makovenko, S. P. Pimentel, D. Vinnikov and J. Martins, "Optimization and implementation of the proportional-resonant controller for grid-connected inverter with significant computation delay," *IEEE Transactions on Industrial Electronics,* vol. 67, no. 2, pp. 1201--1211, 2019.

[18] V. Leite, Â. Ferreira and J. Batista, “Bidirectional vehicle-to-grid interface under a microgrid project,” in *IEEE 15th Workshop on Control and Modeling for Power Electronics (COMPEL)*, 2014.

[19] M. M. Breve and V. Leite, "Control of a Bidirectional Single-Phase Grid Interface for Electric Vehicles," *ICSC-CITIES 2019. Communications in Computer and Information Science,* vol. 1152, 2020.